Chapter 23

Molecular Modeling Studies on Silk Peptides

Stephen A. Fossey and David Kaplan

Biotechnology Division, Natick Research, Development, and Engineering Center, U.S. Army, Natick, MA 01760–5020

A model for the meta-stable state, silk I, of *B. mori* silk fibroin based on conformational energy calculations on representative silk peptides is discussed(*1*). In addition the model and other models for the silk I form are compared with the available experimental data from X-ray and electron diffraction and NMR and IR spectroscopy.

Silk-like proteins are of interest for a number of applications. Among these are high performance fibers (*2*), enzyme immobilizing substrates (*3*) and polymers with highly controlled crystal morphologies (*4*). The last area capitalizes on the ability of genetic means of production to precisely control the primary sequence of the polymer and the self-assembly properties of proteins.

Silk fibroin is a block copolypeptide WITH crystalline domains characterized by a Gly-X repeat where X is Ala or Ser, and of less crystalline domains in which the Gly-X repeat is common but which contain a higher fraction of residues with large side chains(*5*). The crystalline domains of *Bombyx mori* can exist in one of two different morphologies. The more stable one is known as silk II (*6,7*). A detailed structural model for silk II was first proposed by Marsh *et al.* (*8*) and refined by Fraser *et al.* (*9,10*) Its basic feature, a packing of antiparallel, β-pleated sheets, is generally accepted. More recently Takahashi *et al.* (*11*), based on the intensity of X-ray diffraction reflections have proposed that most of the β-sheets in silk fibroin are anti-polar rather than polar as proposed by Marsh *et al.* (see Methods for a description of polar and anti-polar).

Despite a long history of interest in the less stable silk I form it has remained poorly understood. Attempts to induce orientation of the silk I form for studies by X-ray or electron diffraction or solid state NMR cause the silk I form to convert to the more stable silk II form. The silk I form can be obtained by letting the contents of the silk gland dry undisturbed (*9*). If the contents of the gland are mechanically sheared or treated in a number of other ways, the silk II form is obtained (*9,12*).

The sequence of the repeating unit of the crystalline fraction of *B. mori* silk fibroin is (*13*)

$$\text{G-A-G-A-G-S-G-A-A-G[S-G-(A-G)}_n\text{]}_8\text{Y}$$

where n is usually 2 and averages to 2. Poly(L-Ala Gly) has often been used as a model for the crystalline fraction of *B. mori* silk fibroin since the two crystalline forms of poly(L-Ala-Gly) have been shown to be isomorphous with the two crystalline forms of silk.

Experimental studies of silk I have consisted primarily of powder X-ray diffraction (*5,7,14,15*), electron diffraction, (*14*) and solid state ^{13}C-NMR spectroscopy (*12,14-18*). From these studies, it has not been possible to define a unique structure for silk I. Attempts to determine a structure were based on model building and comparison of the predictions of these models with experimental data. A number of models have been proposed, including the "crankshaft" model (*14*) and one based on a loose fourfold helix (*19*).

Conformational energy calculations on representative model polypeptides have been applied to the structure of collagen(*20,21*), poly(glycine) (*22,23*), poly(alanine)(*24*), and copolymers of alanine and glycine (*24*). These efforts have proceeded from model building to comparison with experimental data, but have had some success in elucidating more structural detail than available from experimental results.

Methods

Fossey et al. (*1*) have used conformational energy calculations to investigate the structure of silk-like peptides. The calculations were carried out by using the ECEPP/2 (Empirical Conformational Energy Program for Peptides) algorithm(*25-27*). The details of the calculations have been presented elsewhere, therefore only an overview of the approach is given here.

Starting Conformations. In all cases, β-sheets (regions E and C of Figure 1.) consisting of five strands of six residues, each of alternating alanine and glycine, were studied. The work of Chou *et al.* (*28*) shows that there was little difference in the dihedral angles of sheets composed of either four or eight residues or of two or three strands. The primary effect of increased chain length observed was a slight decrease in the twist generally associated with β-sheets in globular proteins. A six residue peptide was chosen to anticipate the inclusion of serine, which in *B. mori* silk crystalline domains appears once in each six residues. Because of the two fold symmetry of β-strands the sidechains of consecutive residues along the strands project from opposite sides of the β-sheet (*29*). Therefore, in a poly (L-Ala-Gly) strand, all Ala side chains point to the same side. There are then two ways in which adjacent strands can be related. The methyl side chains of the alanine residues in these strands can point to either the same side or to opposite sides of the β-sheet. The sheets in which methyl groups of adjacent strands point to opposite sides of the sheet are referred to as "out-of-register". Those in which all methyl groups point to the same side of the sheet are referred to as "in-register." Takahashi et al. (*11*) have used the nomenclature polar (Figure 2a) and anti-polar (Figure 2b) to refer to in-register and out-of-register respectively, this more common usage will be adopted for the remainder of the paper. Both parallel and antiparallel as well as polar and anti-polar β-sheets were considered. In addition, various packing arrangements for the sheets were considered in the calculations. This approach constitutes a search of conformational space for sheet structures.

Determination of the Unit Cell. To be consistent with prior studies on silk the *b* axis is taken along the strand, the *a* axis is perpendicular to the strand in the plane of the sheet, and the *c* axis is in the direction between sheets. The dimensions of a unit cell correspond to the distance between repeating units in each direction, two residues (Ala-

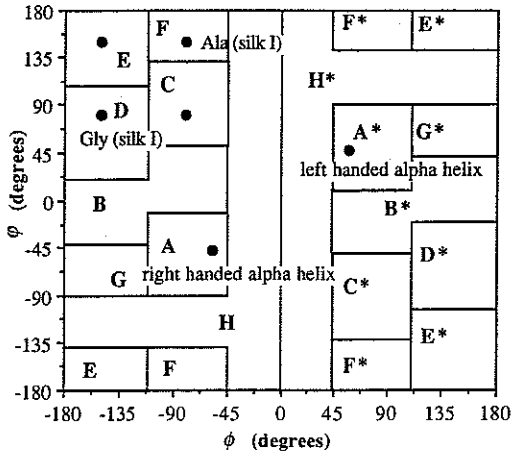

Figure 1. ϕ–φ Map (adapted from ref. 31)

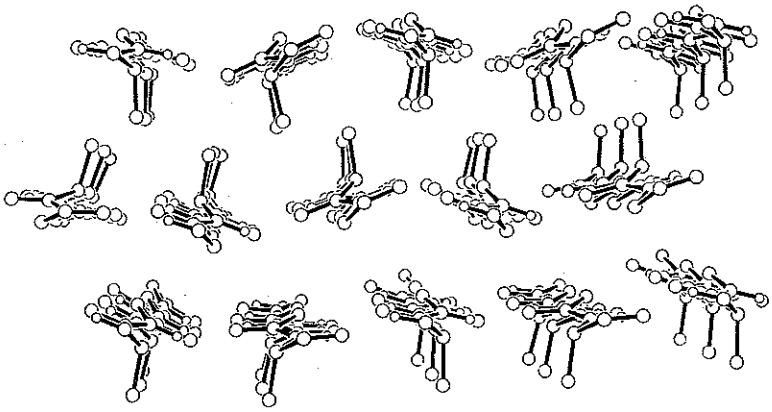

(a)

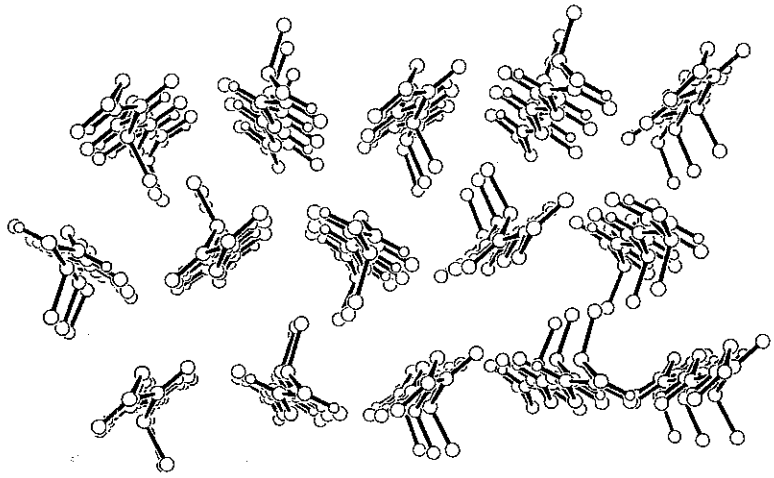

(b)

Figure 2. Silk II (a) polar, (b) anti-polar.

Gly) along the *b* axis and two adjacent chains in the sheet along the *a* axis. In the direction of sheet packing (*c* axis), the repeating unit contains two adjacent sheets for most structures discussed here, with one exception: in the structure referred to later as monoclinic, the repeating unit along the *c* axis contains only one sheet instead of two, because strands in adjacent sheets are identical.

Results

Conformational Energies. All energy-minimized single-sheet structures had a right-handed twist, as found previously (*28,30*). For each of the four types of sheets, energy minima were found in the C and E regions (*31*) of the ϕ–φ map. Figure 1 shows the regions of the ϕ–φ map as well as location of the dihedral angles for the FD conformation. All of those minima that were located in the C region had dihedral angles of approximately (ϕ, φ)=(-80°, 80°) for every residue and all minima located in the E region occurred approximately at (ϕ, φ)=(-150°, 150°) for every residue. In addition to these two minima, the anti-polar arrangement for an antiparallel sheet gave a third minimum with a different conformation, in which most of the alanyl residues adopted dihedral angles near (ϕ, φ)=(-80°, 150°) and most of the glycyl residues adopted dihedral angles near (ϕ, φ)=(-150°, 80°) . The components of the conformational energy and the characteristic repeats of each single sheet minimum are shown in Table I.

Table I.
Conformational Energies (kcal/mol) of Single Sheets

Descriptor[a-c]	Total	Inter-Strand	Intra-Strand	Repeat Distance Along Chain	Repeat Distance Across Direction (nm)
E, A, Polar	-73.4	-121.3	47.9	0.713	0.480
C, A, Polar	-91.1	-108.0	16.9	0.566	0.459
E, P, Polar	-43.1	-90.9	47.8	0.715	0.460
C, P, Polar	-91.9	-107.7	15.7	0.563	0.456
E, A, A-Polar	-76.8	-128.4	51.7	0.708	0.459
C, A,A-Polar	-104.8	-115.5	10.6	0.566	0.460
FD, A, A-Polar	-79.9	-133.6	53.8	0.645	0.449
E, P, A-Polar	-72.1	-125.8	53.7	0.716	0.448
C, P, A-Polar	-90.2	-105.4	15.2	0.567	0.483

SOURCE: Adapted from ref. 1.
a The letter code of Zimmerman et al.(*31*) is used. FD indicates conformations near (ϕ, φ) = (-80°,150°) for Ala, (ϕ, φ) = (-150°,80°) for Gly. For the other structures, the letter code pertains to the conformational states of both Ala and Gly (see Figure 1).
b A: antiparallel sheet; P: parallel sheet.
c Polar (in-register) sheet; A-Polar: anti-polar (out-of-register) sheet.

For both the polar and anti-polar single sheets, the minima in the C region are clearly of lower energy. From the intra- and interchain components of the energy, it can be seen that the minima in the C region are favored because of a much lower intrachain energy.

This lower intrachain energy is the result of the formation of a bent intrachain hydrogen bond in the C conformation, while interstrand hydrogen bonds are also retained (*32,33*). The minima in the C region show poor agreement with the crystal lattice repeats found experimentally for the two crystalline forms of poly(L-Ala-Gly). The disagreement disappears, however, when the energy of three stacked sheets is considered, as discussed below.

Conformational Energies of Three Stacked Sheets. Table II lists the conformational energy contributions for stacked β-sheets. The C-region minima are not listed because their total energy is much higher by at least 300 kcal/mol (*i.e.* at least about 3 kcal/ mol of residues). Although the isolated sheets with C conformations contain short interstrand hydrogen bonds, in addition to the bent intrachain hydrogen bonds as mentioned above (*32,33*), many of these interstrand hydrogen bonds are weakened or broken when the energies of the stacked sheets are minimized.

Table II.
Conformational Energies (kcal/mol) of Three Stacked Sheets

Number	Description[a-c]	Total	intra-strand	inter-strand[d]	inter-sheet
1e	E, A, Polar	-481	164	-297	-348
2f	E, A, Polar	-437	152	-338	-251
3	E, P, Polar	-420	153	-390	-183
4	E, A, A-Polar	-299	152	-334	-117
5g	FD, A, A-Polar	-394	177	-387	-184
6h	FD, A, A-Polar	-388	191	-189	-390
7	E, P, A-Polar	-260	155	-226	-189

SOURCE: Adapted from ref. 1.
a-c See corresponding footnotes of Table I. d Sum of interstrand energies between strands of the same sheet. e Figure 2a. f Unlike the other polar structures, these sheets have Gly faces stacked against Ala faces of adjacent sheets. g Orthorhombic structure, Figure 3a. h Monoclinic structure, Figure 3b.

The computed lowest energy structure is formed by antiparallel β-sheets with polar chains and residues in the E conformational state (line 1 in Table II). As discussed below, this structure is essentially identical with the model that had been proposed by Marsh *et al.* (*8*) and its unit cell parameters agree with the observed values for silk II and the silk II like structure of poly(L-Ala-Gly). The lowest energy anti-polar structure is composed of antiparallel sheets in which the residues adopt the dihedral angles alternating near (ϕ, φ)=(-80°,150°) for Ala and near (ϕ, φ)=(-150°, 80°) for Gly (Figure 1). These dihedral angles correspond to right-handed and left-handed twisting of sheets (*34*), respectively, with approximately equal magnitudes of the twist. Their alternation results in a twofold axial repeat, with no net twist of the sheets. This structure can exist as two variations with slightly different packing arrangements that differ in total energy by only 6 kcal/mol. or <0.1 kcal/mol of residues (lines 5 and 6 in Table II).

The higher energy modification of the anti-polar structure (line 6 of Table II) has a monoclinic unit cell (Figure 3b). The dihedral angles of the orthorhombic and

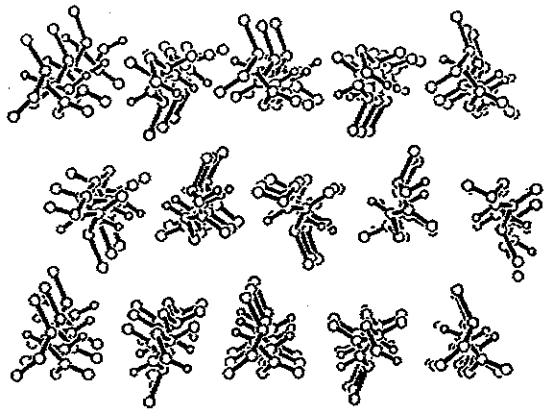

(a)

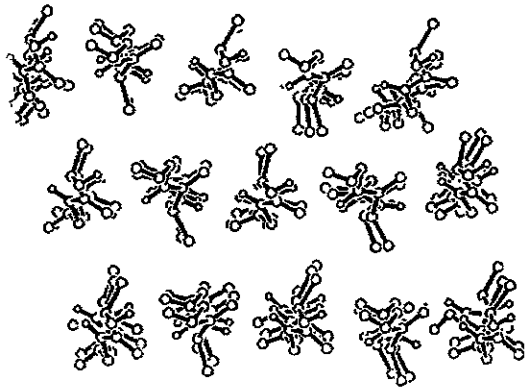

(b)

Figure 3. Silk I (a) orthorhombic, (b) monoclinic (adapted from ref 1).

monoclinic modifications are very close to each other, differing on the average by less than 2°. The unit cell dimensions in the plane of the sheets (axes *a* and *b*) are within 0.01 nm of each other. Because of the change in the intersheet packing, however, the lengths of the *c* axes differ in the two structures. The length of the c axis in the monoclinic structure is 0.595 nm, inclined at the unit cell angle $\beta = 106.6°$, *i.e.* the distance between second nearest-neighbor sheets is 1.190 nm, measured along the *c* axis, in contrast to the corresponding *c* axis length of 1.126 nm in the orthorhombic structure. The unit cell geometry in the monoclinic structure, on the other hand, results in a perpendicular separation of 1.14 nm between second-neighbor sheets, which is only slightly higher than the 1.126 nm distance in the orthorhombic structure. The $c = 1.126$ nm unit cell dimension of the orthorhombic structure agrees better with observed X-ray data, as shown below. For these reasons, and because of the difference in energies, we propose the orthorhombic modification as the model for silk I, as discussed below. However, given that the two structures are quite close in energy it seems reasonable that both variations would be observed as a disordered packing of sheets.

The energy of the polar silk II structure (line 1 of Table II) is 87 kcal/mol lower than that of the proposed anti-polar silk I structure (line 5 of Table II), *i.e.* it is lower by almost 1 kcal/mol of residues. This suggests why silk II is more stable than silk I, as observed experimentally. On the other hand, the energy difference is sufficiently small, so that silk I can exist as a less stable form.

Comparing Tables I and II, it can be seen that the order of the energy minima is different for single and for stacked sheets. Two differences are of particular note. First, if one considers only conformational states E and FD, the differences in the total energy are dominated in both cases by the interstrand component, but the intersheet energy may also make a large contribution in some structures. In the single sheet, anti-polar chains are favored over polar ones in the E conformation by the interstrand energy, because the strands can be packed more closely, allowing an interchain spacing of 0.46 nm (as compared to 0.48 nm for in-register antiparallel sheets). On the other hand, for stacked sheets, an antiparallel polar sheet with an E conformation (line 1 of Table II) has the lowest energy. It is favored over anti-polar sheets, because the low intersheet energy, arising from interactions of two Gly faces in contact with each other and of two Ala faces in contact with each other, more than compensates for the less favorable intrasheet chain-chain interactions. This is seen by a comparison of lines 1 and 2 of Table II, where it is indicated that the stacking of like faces in contact (line 1) is highly favored by over 100 kcal/mol in intersheet energy over the arrangement in which the Gly faces pack against Ala faces (line 2). Second, conformational states FD and E have nearly the same total energy in antiparallel anti-polar single sheets (Table I), but the FD state allows better stacking, as indicated by the much more favorable intersheet energies (*cf.* line 4 with lines 5 and 6 of Table II).

Discussion

The comparison of the low energy structures with the available experimental data is discussed below. The low energy polar antiparallel form corresponds to a β-pleated sheet (with a structure similar to silk II) (*8*). Fossey *et al.* (*1*) proposed, based on a comparison with X-ray and electron diffraction data as well as the calculated density, that the anti-polar antiparallel sheet with dihedral angles which differ from those of a beta sheet should serve as a model for silk I.

Poly(L-Alanine-Glycine), Silk I Form. The structure proposed by Fossey *et al.* (*1*), shown in Figure 3a, is a hydrogen-bonded antiparallel sheet in which the alanyl residues adopt dihedral angles near

(ϕ, φ)=(-80°, 150°) and the glycyl residues adopt dihedral angles near (ϕ, φ)=(-150°, 80°) (Table III). Since the proposed structure is composed of anti-polar chains, the methyl side chains of alanyl residues in adjacent strands point to opposite sides of the sheet. The side-chain distribution in the anti-polar sheet is thus symmetrical, in contrast to the polar silk II form, which has all alanyl residues on one side and all glycyl residues on the other. The sheets in both forms are stacked such that the strands of adjacent sheets are offset laterally (*i.e.* horizontally in Figure 3) by one half the interstrand distance (*9*).

Table III.
Observed and Calculated Unit Cell Dimensions for Poly(L-Ala-Gly) Silk II Form

Unit Cell Axes (A)[a]	Observed[b]	This Work[c]	Colonna-Cesari *et al.*[d]
a	9.44	9.48	(9.44)
b	6.94	7.06	(6.94)
c	8.96	8.66	8.72
Intersheet[e] spacings (A)			
Ala-*c*	5.17	5.02[f]	5.02
Gly-*c*	3.79	3.72[f]	3.70

SOURCE: Adapted from ref. 1.
a The labeling of the unit cell axes, as used in various publications, refers to different directions for the two forms of silk, in relation to the sheet structure. The notation used here follows the notntion for silk II, as described in Methods.
b Reference 4, p. 312, and Ref. 5.
c Structure 1 of Table II, shown in Figure 2a.
d Reference 24. In this calculation, the *a* and *b* axes were held fixed at their observed values (shown in parentheses), and only the c axis was allowed to vary. For the parameter *a*, an interstrand distance of 4.72 A was used in Ref. 24. The doubled value, correspondlng to the *a* axis of the unit cell, is listed here.
e Ala-*c* is the spacing in the *c* direction across Ala-Ala faces of stacked sheets; Gly-*c* is the spacing across Gly-Gly faces of stacked sheets.
f The intersheet spacing is calculated as an average distance of the C^{α}'s of the top and bottom sheets from a least-squares plane that was fit to the C^{α} atoms of the middle sheet.

There are two crystalline forms of the proposed silk I sheets, one in which the unit cell is orthorhombic with $a = 0.894$ nm, $b = 0.646$ nm, $c = 1.126$ nm. The *a* dimension is twice the interstrand distance, the *b* dimension is the repeat for two residues along the chain, and the c dimension is twice the intersheet distance. The other is a monoclinic unit cell with $a = 0.894$ nm, $b = 0.646$ nm and $c = 1.213$ nm and $\beta = 106.6°$. The observed spacings reported by Lotz and Keith (*14*) are consistent with both unit cells. Table IV shows the corresponding spacings for the orthorhombic unit cell.

Table IV.
Observed and Calculated Spacings for the Silk I Form of Poly(L-Ala-Gly) and Silk I

Poly(L-Ala-Gly) in the Silk I Form[a]		Silk I[b]		calculated structure
spacing(nm)	intensity[c]	spacing (nm)	intensity[c]	spacing (nm)
0.780	w-d			
0.721	s	0.729	ms	0.700
0.560	w-d	0.561	w	0.563
0.486	w-d	—	—	
0.449	vs	0.450	s	0.447
0.420	w-d	—	—	
0.394	ms	0.402	w	0.375
0.360	ms	0.362	ms	
0.316	ms-vd	0.315	ms	0.323
0.272	w-d	0.273	w	0.282
0.240	ms-vd	0.244	mw	
0.225	vw-d	0.224	vw	0.225
0.207	vw-d	—	—	

SOURCE: Adapted from ref. 1.
a Reference 14.
b Reference 15.
c Abbreviations used: w, weak; d, diffuse; s, strong; vs, very strong; ms, medium-strong; vw, very weak; vd, very diffuse.

The hydrogen bonds in the proposed structures are of normal length, with an average H • • • O distance of 0.195 nm. The average N—H • • • O angle of 154° is close to those in observed antiparallel beta-sheets of globular proteins(*35*), 160° ± 10°, and it is the same as the value of 154° reported(*36*) for β-poly(L-Ala). The average C=O • •H angle is 134°, which is less than the 158° reported for β-poly(L-Ala). The out-of-plane component of the C = O • • • H angle is 39°, which is considerably larger than the median of the absolute value of the out-of-plane angle, 15°, in antiparallel, β-sheets (*35*). However, in small molecules there is considerable variation in the C = O • • • H angle, with large out of-plane angles being common. In fact, the preferred C = O • • • H angle is 135° in many crystals of small molecules, which are free to adopt the most advantageous geometry (*35*). The hydrogen bonds formed in the proposed structure are thus somewhat different from those observed in a β-pleated sheet, but they appear to be reasonable, in comparison with hydrogen bonds observed in organic crystals (*35*).

The X-ray diffraction results of Asakura *et al.* (*15*) for silk I and Lotz and Keith (*14*) for the silk I form of poly(L-Ala-Gly) are shown in Table IV, in comparison with the characteristic repeat distances from the proposed structure. From X-ray or electron diffraction, two lattice dimensions are characteristic of the silk I form (*14*); in a third, the repeat is less certain. We assign the strong observed reflection at 0.45 nm to the interstrand distance. The average interstrand spacing in our model is 0.447 nm. The computed fiber axis repeat is 0.646 nm for two residues or 0.323 nm per residue, close to the observed 0.316 nm reflection. A spacing of 0.700 nm in our model corresponds to a strong reflection indexed as 101. This spacing is closest to the observed 0.721 nm

spacing for poly (L-Ala-Gly). Given that the ECEPP/2 potential produces a shorter intersheet distance for the silk II form than the observed spacing this seems to be a reasonable match. Thus, most of the observed reflections, especially the strong ones, can be indexed in a consistent manner using the model proposed here (Table IV). The calculated density of the overall structure is 1.30 g/cm^3 while Lotz and Keith (*14*) report that the density of wet crystals of poly(L-Ala-Gly) in the silk I form is 1.33 g/cm^3, and when corrected for water content, 1.25 g/cm^3.

A number of models for silk I have been proposed earlier. In the "crankshaft model" of Lotz and Keith (*14*), the alanyl residues are in a β-sheet conformation and the glycyl residues in a left-handed α-helical conformation. The resulting unit cell has the dimensions a = 0.472 nm, b = 0.96 nm, and c = 1.44 nm.A fiber axis repeat of an integer multiple of 0.32 nm has been proposed by Lotz and Keith (*14*). Using the crankshaft model, they assigned to the length of the unit cell the value of 0.96 nm, *i.e.* four residues per chain axis repeat. In the model proposed here, b = 0.646 nm, i.e., an average axial rise of 0.323 nm per residue accounts well for this reflection. When potential disorder, which eliminates or reduces certain reflections, is taken into account the crankshaft model provides a good fit to the X-ray diffraction spacings and intensities.

We have also calculated the conformational energy of three sheets of five strands of the antiparallel crankshaft structure proposed by Lotz and Colonna Cesari (*37*). The total energy was -365 kcal/mol., which is considerably higher than the values computed for our model (Table II). The structure proposed by Lotz and Keith's(*14*) and the one presented here are alternative models for silk I, because both are consistent with the fiber X-ray diffraction data.

There is also structural information from infrared and NMR spectroscopy available. Brack and Spach (*38*) observed IR spectra which corresponded to neither an α nor a β form. While the crankshaft model has alanine residues in a β-sheet conformation and glycine residues in an α-helical conformation. Additionally, the NH stretching mode is split into two frequencies (3280 cm^{-1} and 3315 cm^{-1}) which Lotz and Keith (*14*) suggest could be attributed to two hydrogen bond geometries. Two hydrogen bond geometries require that both parallel and antiparallel sheet arrangements be present. The silk I model of Fossey *et al.* (*1*) has two hydrogen bond geometries based on the relation of the hydrogen bond to the peptide plane of the residues, but it has not been shown that this would account for the splitting observed.

A number of workers have published NMR data which is relevant to the crystal structure of silk. Using ^{13}C NMR Saito *et al.* (*19*) conclude that the alanine residues of silk I cannot be in the β-sheet conformation as in the crankshaft model. Asakura *et al.* (*39*) using [1-^{13}C]Gly labeled *B. mori* fibroin in solution measured the long range coupling constant $^3J_{C'\text{-}N\text{-}C^{\alpha}\text{-}H}$. These coupling constants were then converted by the Karplus-like relation of Bystrov (*40*) to obtain the dihedral angle φ for alanine and serine residues. The values of φ allowed are -143° to -147°, -93° to -97°, -4° to -6°, and 124° to 126°. Since the silk I form is obtained by drying silk solutions with out disturbance the silk I conformation is probably quite close to solution conformation. The φ value for alanine in the crankshaft model is -124° and -104° while in the model of Fossey *et al.*. (*1*) it is -80°. Recently, Nicholson *et al.* (*41*) have reported solid state NMR measurements for the silk II form. Unfortunately the oriented samples needed cannot be obtained for silk I. Although these data are not definitive they do tend to support the model of Fossey *et al.* (*1*) over the crankshaft model.

Several other models have been proposed in which the chains adopt various helical conformations (*42-45*). It has been shown for several models (*14,37,42,44*) by conformational energy computations that their strand conformations correspond to relatively low-energy conformations of an isolated poly(L-Ala-Gly) chain. Most of these models lead to less consistent assignments of the available experimental diffraction data with regard to the translational repeat than those of the present model.

Silk I to Silk II Transition. The proposed silk I model has a low intrachain energy barrier for the conversion to the silk II form. To form the polar model of silk II requires the breaking and reforming of all hydrogen bonds and rotation of every other chain by 180° around the chain axis. Interestingly, to form the anti-polar silk II form doesnot require breaking any hydrogen bonds or chain rotations. This lower energy barrier could account for the increased population of antipolar silk II, as proposed by Takahashi (*11*), despite the fact that the polar form has a lower conformational energy.

Summary

A model for silk I and the silk I form of poly(L-alanine-glycine) has been proposed by Fossey et al (*1*), based on conformational energy calculations. The computed silk model provides good agreement with the available experimental data, because it can account for most spacings in the observed fiber X-ray diffraction pattern of silk I and of the corresponding form of poly(L-Ala-Gly). The alanyl residues adopt a right handed sheet-like conformation and the glycyl residues a left-handed sheet-like conformation in the proposed structure. The dimensions of its orthorhombic unit cell are $a = 0.894$ nm, $b = 0.646$ nm, and $c = 1.126$ nm. Silk fibroin, when in the gland, is a concentrated solution, and when it is allowed to dry undisturbed, is found to be in the silk I form (*5*), therefore, it is likely that the liquid crystalline structures also consist of silk I. The proposed silk I model may also represent the structure of the liquid crystal phase recently described by Kerkam *et al.* (*46*), who showed that concentrated silk fibroin solutions formed nematic liquid crystals.

LITERATURE CITED

1. Fossey, S. A.; Nemethy, G.; Gibson, K. D.; Scheraga, H. A. *Biopolymers* **1991,** *31*,1529.
2. Lombardi, S. J.; Fossey, S. A.; Kaplan, D. K. Proceedings of the American Society for Composites - Fifth Technical Conference. **1991**
3. Demura, M.; Asakura, T. *Biotech. and Bioeng.* **1989,** *33*, 598.
4. McGrath, K. P.; Fournier, M. J.; Mason, T. L.; Tirrel, D. A. *J. Am. Chem. Soc.* **1992,** *114*, 727.
5. Fraser, R. D. B.; MacRae, T. P. *Conformation in Fibrous Proteins and Related Synthetic Polypeptides,* Academic Press: New York, NY, 1973; Chapt. 13.
6. Kratky, O.; Schauenstein, E.; Sekora, A. *Nature* **1950**, *165*, 319.
7. Kratky, O. *Trans. Faraday Soc.* **1956,** *52*, 558.
8. Marsh, R. E.; Corey, R. B.; Pauling, L. *Biochem. Biophys. Acta* **1955**, *16*, 1.
9. Fraser, R. D. B.; MacRae, T. P.; Stewart, F. H. C.; Suzuki, E. *J. Mol. Biol.* **1965**,*11*, 706.
10. Fraser, R. D. B.; MacRae, T. P.; Stewart, F. H. C. *J. Mol. Biol* **1966,** *19,* 580.
11. Takahashi, Y.; Gehoh, M.; Yuzuriha, K. *J. Poly. Sci. Pt. B: Poly. Phys.* **1991,** *29,* 889.
12. Ishida, M.; Asakura, T.; Yokoi, M.; Saito, H. *Macromolecules* **1990**, *23*, 88.
13. Strydom, D. J.; Haylett, T.; Stead, R. H. *Biochem. Biophys. Res. Comm.* **1977**, *79*, 932.

14. Lotz, B.; Keith, H. D. *J. Mol. Biol.* **1971**, *61*, 201.
15. Asakura, T.; Kuzuhara, A.; Tabeta, R.; Saito, H. *Macromolecules* **1985**, *18*, 1841.
16. Kricheldorf, H. R.; Muller, D.; Ziegler, K. I *Polymer Bull.* **1983**, *9*, 284.
17. Saito, H.; Tabeta, R.; Kuzuhara, A.; Asakura, T. *Bull. Chem. Soc. Japan* **1986**, *59*, 3383.
18. Asakura, T.; Yoshimizu, H.; Yoshizawa, F. *Macromolecules* **1988**, 21, 2038.
19. Saito, H.; Tabeta, R.; Asakura, T.; Iwanaga, Y.; Shoji, A.; Ozaki, T.; Ando, I. *Macromolecules* **1984**, *17*, 1405.
20. Scheraga, H. A.; Nemethy, G. In *Molecules in Natural Biosciences—Encomium for Linus Pauling*, **1991**.
21. Nemethy, G. & Scheraga, H. A. *Bull. Inst. Chem. Res. Univ. Kyoto* **1989**, *66*, 398-408.
22. Lotz, B. *J. Mol. Biol.* **1974**, *87*, 169.
23. Colonna-Cesari, F.; Premilat, S.; Lotz, B. *J. Mol. Biol.* **1974**, *87*, 181.
24. Colonna-Cesari, F.; Premilat, S.; Lotz, B. *J. Mol. Biol.* **1975**, *95*, 71.
25. Momany, F. A.; McGuire, R. F.; Burgess, A. W.; Scheraga, H. A. *J. Phys. Chem.* **1975**, *79*, 2361.
26. Nemethy, G.; Pottle, M. S.; Scheraga, H. A. *J. Phys. Chem.* **1983**, *87*, 1883.
27. Sippl, M. J.; Nemethy, G.; Scheraga, H. A. *J. Phys. Chem.* **1984**, *88*, 6231.
28. Chou, K.-C.; Pottle, M.; Nemethy, G.; Ueda, Y.; Scheraga, H. A. *J. Mol. Biol.* **1982**, *162*, 89.
29. Pauling, L.; Corey, R. B. *Proc. Natl. Acad. Sci., U.S.A.* **1953**, *39*, 253.
30. Chou, K.-C.; Nemethy, G.; Rumsey, S.; Tuttle, R. W.; Scheraga, H. A. *J. Mol. Biol* **1986**, *188*, 641.
31. Zimmerman, S. S.; Pottle, M. S.; Nemethy, G.; Scheraga, H. A. *Macromolecules* **1977**, *10*, 1.
32. Chou, K.-C.; Scheraga, H. A. *Proc. Natl. Acad. Sci., U.S.A.* **1982**, *79*, 7047.
33. Chou, K.-C.; Nemethy, G.; Scheraga, H. A. *J. Mol. Biol.* **1983**, *168*, 389.
34. Chou, K. C.; Nemethy, G.; Scheraga, H. A. *Accts. Chem. Res.* **1990**, *23*, 134.
35. Baker, E. N.; Hubbard, R. E. *Prog. Biophys. Mol. Biol.* **1984**, *44*, 97.
36. Arnott, S.; Dover, S. D.; Elliot, A. *J. Mol. Biol.* **1967**, *30*, 201.
37. Lotz, B.; Colonna-Cesari, F. *Biochimie* **1979**,*61*, 205.
38. Brack, A.; Spach, G. *Biopolymers* **1972**, *11*, 563.
39. Asakura, T.; Wanatabe, Y.; Itoh, T. *Macromolecules* **1984**, *17*, 2421.
40. Bystrov, V. F. *Prog. NMR Spectrosc.* **1976**, *10*, 41.
41. Nicholson, L. K.; Asakura, T.; Demura, M.; Cross, T. A. *Biopolymers* **1993**, *33*, 847.
42. Konishi, T.; Kurokawa, M. *Sen-i Gakkaishi* **1984**, *24*, 550.
43. Asakura, T.; Yamaguchi, T. *J. Seric. Sci. Jpn.* **1987**, *56*, 300.
44. Ichimura. S.; Okuyama, K. *Polym. Prep. Jpn.* **1989**, *38*, E48.
45. Oka, M.; Baba, Y.; Kagemoto, A.; Nakajima, A. *Polym. J. (Jpn.)* **1990**, *22*, 416.
46. Kerkam, K.; Viney, C.; Kaplan, D.; Lombardi, S. *Nature* **1991**, *349*, 596.

RECEIVED July 15, 1993